An alternative neutron diffractometer performance for strain/stress measurements

Pavol Mikula,[a] Jan Saroun, Vasyl Ryukhtin, and James Stammers
Neutron Physics Department, Nuclear Physics Institute Czech Academy of Sciences, Rez, Czech Republic

(Received 17 March 2020; accepted 29 April 2020)

An alternative neutron diffractometer performance, which documents the feasibility of using a high-resolution three-axis neutron diffractometer for elastic and plastic deformation studies of bulk metallic polycrystalline samples, is presented. Contrary to the conventional double-axis setting, the suggested alternative consists of an unconventional three-axis set-up employing a bent perfect crystal monochromator and an analyzer with a polycrystalline sample in between. Though the alternative is, for measurements, much more time-consuming, its sensitivity to the change of the diffraction angle of the sample is, however, substantially higher and permits also plastic deformation studies on the basis of analysis of the diffraction line profiles. Moreover, much larger widths (up to 10 mm) of the irradiated gauge volumes can be investigated when just slightly affecting the angular resolution properties of the experimental setting. © *2020 International Centre for Diffraction Data.*
[doi:10.1017/S0885715620000329]

Key words: neutron diffraction, Bragg diffraction optics, strains

I. INTRODUCTION

The principle of the neutron diffraction method consists in the precise determination of the d_{hkl} spacing of particularly oriented crystal planes (hkl). In neutron and X-ray diffraction, the angular positions of the diffraction maxima are determined by the well-known Bragg condition $2d_{hkl} \cdot \sin \theta_{hkl} = \lambda$ (θ_{hkl} – Bragg angle, λ – the neutron wavelength). It offers a unique nondestructive technique for the determination of the strain/stress fields. When defining the elastic strain ϵ as $\epsilon = \Delta d/d_{0,hkl}$, it means that it is, in fact, a relative change of the lattice spacing d_{hkl} with respect to the strain-free value of the lattice spacing $d_{0,hkl}$. The strain within a material is a tensor, and in a single diffraction measurement of strain, one obtains just the vector component parallel to the scattering vector $\boldsymbol{Q}$ which is perpendicular to the reflecting set of planes (see Figure 1). For other strain components, other geometrical positions of the sample need to be chosen. It follows from the definition of the strain ϵ that the knowledge of the $d_{0,hkl}$ value is a crucial task (Noyan and Cohen, 1987; Hutchings and Krawitz, 1992; Stelmukh *et al.*, 2002). After the differentiation of the Bragg condition, we arrive at a simple formula $\epsilon = -\cot \theta_{hkl} \cdot \Delta\theta_{hkl}$. This formula indicates that strain ϵ gives rise to a change in the scattering angle $2\theta_{hkl}$ resulting in an angular shift $\Delta(2\theta_{hkl})$ of the scattering angle (for particular reflecting planes illuminated by a fixed wavelength). Therefore, from the shift in the Bragg angle $\Delta\theta_{hkl}$ (relative to that of the stress-free material), it is possible to determine the average lattice macrostrain over the irradiated gauge volume. After obtaining three strain components from the measurement on, e.g., a steel sample, the conversion of strains to stresses is carried out by means of the relation

$$\sigma_x = \frac{E_{hkl}}{(1-2\nu_{hkl})(1+\nu_{hkl})}[(1-\nu_{hkl})\varepsilon_x^{hkl} + \nu_{hkl}(\varepsilon_y^{hkl} + \varepsilon_z^{hkl})] \quad (1)$$

where $\varepsilon_{x,y,z}^{hkl}$ is the x,y,z components of the lattice strain measured at the hkl crystal lattice planes, E_{hkl} and ν_{hkl} are the diffraction elastic Young modulus and diffraction Poisson ratio, respectively. The neutron strain/stress scanner, which is in fact a powder diffractometer equipped with a position sensitive detector (PSD), evaluates the variations of lattice spacing within a sample. The required spatial resolution is usually of the order of millimeters and is determined by the dimensions of the gauge volume. The scanner is usually equipped with a bent perfect crystal (BPC) monochromator and optimized with respect to luminosity and resolution in a limited range of scattering angles $2\theta_S$ (Noyan and Cohen, 1987; Hutchings and Krawitz, 1992; Stelmukh *et al.*, 2002). The instrument can be also equipped with an external loading machine as, e.g., with a tension/compression rig (see Figure 2).

II. HIGH-RESOLUTION THREE-AXIS DIFFRACTION SETTING

Conventional two-axis neutron scanners usually use, for strain determination, beam optics elements, namely focusing and optimally bent monochromator, a system of slits before and after the sample creating a gauge volume element (irradiated by the beam coming from the monochromator) and a PSD imaging the diffraction profile coming from the irradiated gauge volume (Mikula *et al.*, 1996, 1997; Seong *et al.*, 2011). The resolution of the conventional scanner is thus determined mainly by the thickness and curvature of the monochromator, monochromator take-off angle, the widths

[a]Author to whom correspondence should be addressed. Electronic mail: mikula@ujf.cas.cz

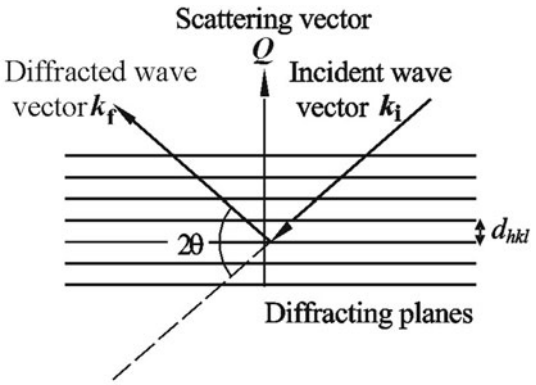

Figure 1. Schematic sketch of the Bragg diffraction geometry.

of the slits (usually in the order of 1–3 mm), the divergence of the beam diffracted by the gauge volume, and the spatial resolution of PSD. The combination of all these features results in an uncertainty (*FWHM* of the diffraction peak profile image as recorded on the PSD) of about roughly 10^{-3} rad which appears still sufficiently small for the measurement of $\Delta(2\theta_{hkl})$ angular shifts brought about by strains. However, the mentioned resolution is not sufficient for measurements of changes of diffraction line profiles imaged by PSD which would permit the carrying out of microstrain and grain size studies for plastically deformed polycrystalline samples.

Rather a long time ago, first attempts with a high-resolution three-axis setting as schematically shown in Figure 3(a) were tested (Vrána *et al*., 1994; Macek *et al*., 1996; Hirschi *et al*., 1999). Following the sketch displayed in Figure 3(a) (for small widths of the samples), a maximum resolution from this arrangement can be achieved for minimal dispersion of the whole system. When treating it in momentum space, this means that the orientation of the Δk domains related to the monochromator and the analyzer are matched to that of the sample. For $L_{MS}/(R_M \cdot \sin\theta_M) \neq 1$ and $L_{SA}/(R_A \cdot \sin\theta_A) \neq 1$, a general form for focusing in momentum space (not dependent on α_1 and α_2), which minimizes the dispersion between all elements, can be derived as (Vrána *et al*., 1994)

$$2\tan\theta_S = \frac{\tan\theta_M}{1 - L_{MS}/(R_M \cdot \sin\theta_M)} + \frac{\tan\theta_A}{1 - L_{SA}/(R_A \cdot \sin\theta_A)}. \quad (2)$$

When fulfilling the condition (2), a maximum peak intensity and a minimum *FWHM* of the analyzer rocking curve can be expected. However, it should be pointed out that in some cases, it is difficult to fulfill it. Of course, this high-resolution performance can be used for macro-strain scanning, but due to the step-by-step analysis with the analyzer, the measurement would be impractical as a result of rather low detector signal.

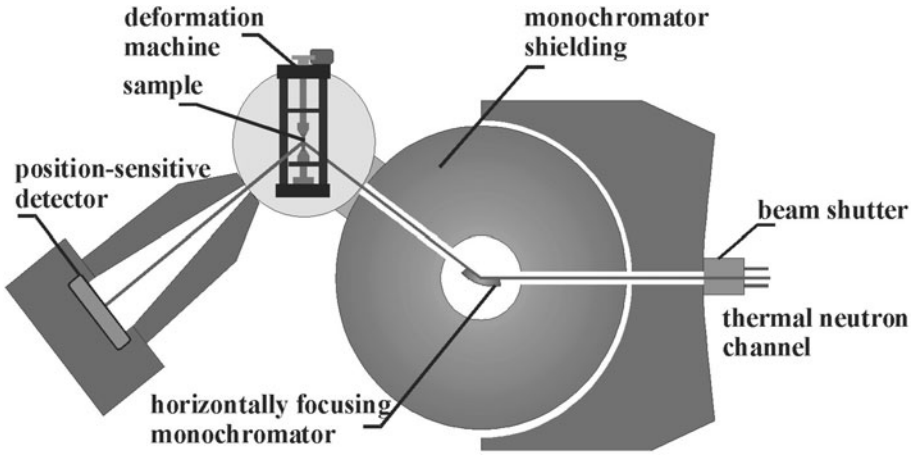

Figure 2. Conventional strain scanner with a tension/compression rig.

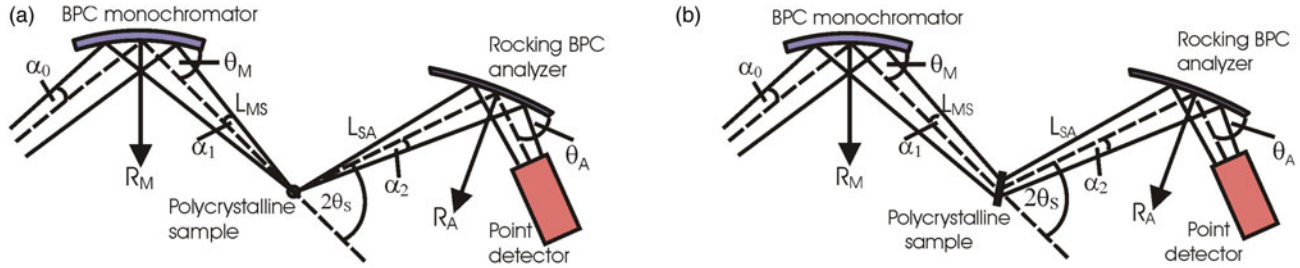

Figure 3. Three axis diffractometer settings employing the BPC monochromator and the analyzer as used in the feasibility studies (R_M, R_A – radii of curvature, θ_M, θ_A – Bragg angles) for vertical (a) and horizontal (b) positions of a polycrystalline sample of the cylindrical form.

https://doi.org/10.1017/S0885715620000329 Published online by Cambridge University Press

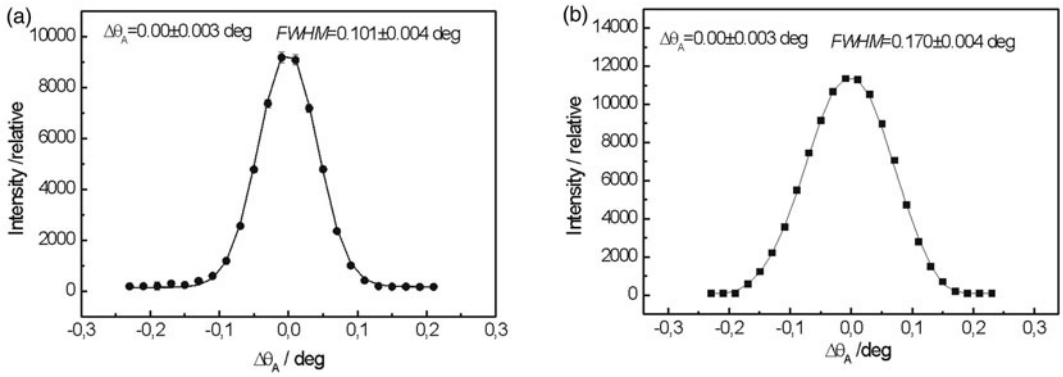

Figure 4. Analyzer rocking curves for the virgin α-Fe(110) sample situated on the second axis of the instrument in the vertical (a) and horizontal position (b).

However, due to its high resolution, it can be used for plastic strain studies on the basis of diffraction profile analysis as, e. g., in deformation studies on samples under the external thermo-mechanical load (Vrána *et al*., 1994; Macek *et al*., 1996; Hirschi *et al*., 1999). Recently, it has been found that the setting provides a sufficiently high resolution, though slightly relaxed, when wider slits (e.g. of the width of about 10 mm) or wider samples are used as schematically shown in Figure 3(b). If the same step-by-step analysis were to be applied, the principal drawback, being that of the time taken for such a measurement, would be smaller because the detector signal could be much higher due to the larger horizontal dimension of the sample. It is well known that the vertical direction has a negligible influence on the resolution. The experimental tests were carried out on the three-axis neutron diffractometer installed at the Řež research reactor LVR-15. Si(111)-monochromator and Ge(311)-analyzer single crystals had the dimensions of $200 \times 40 \times 4$ mm^3 and $20 \times 40 \times 1.3$ mm^3 (length × width × thickness), respectively. The monochromator Si(111) set for take-off angle of $2\theta_M = 29.95°$ and providing the neutron wavelength of 0.162 nm had a fixed curvature with the radius R_M of about 12 m. The Ge(311) analyzer with the nominal diffraction angle of $\theta_A = 28.39°$ had a changeable radius of curvature R_A in the range from 3.6 to 36 m. Figure 4 demonstrates the difference in the resolution represented by *FWHM* of the analyzer rocking curve for two positions (vertical and horizontal) of the α-Fe(110) standard sample of the diameter of 5.1 mm. The radius of curvature of the analyzer was $R_A = 9$ m when the dispersion of the whole setting was minimized. In this case, only one Cd slit having a window of 2×1 cm^2 (height × width) was used. In the next step, a plastically deformed sample of the same

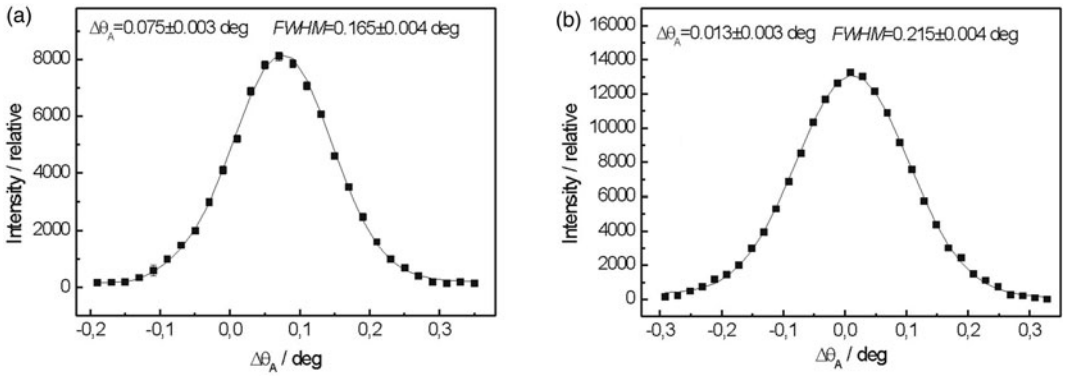

Figure 5. Analyzer rocking curves for the deformed α-Fe(110) sample in the vertical (a) and horizontal position (b).

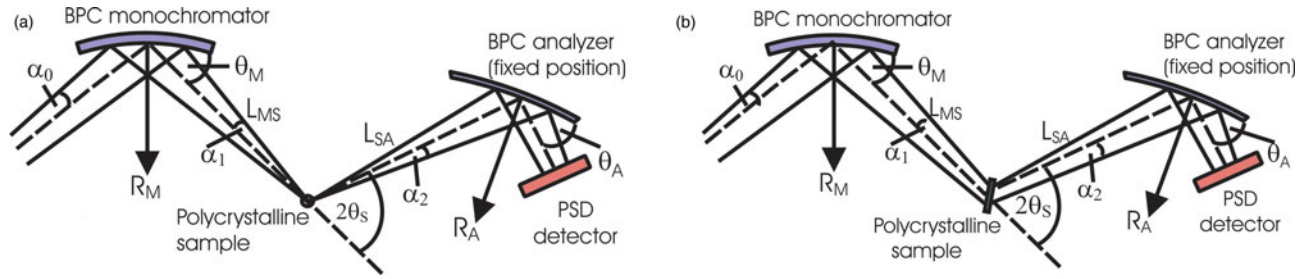

Figure 6. Three-axis diffractometer alternative with the fixed position of the analyzer in combination with the PSD detector for vertical (a) and horizontal (b) positions of the polycrystalline sample.

https://doi.org/10.1017/S0885715620000329 Published online by Cambridge University Press

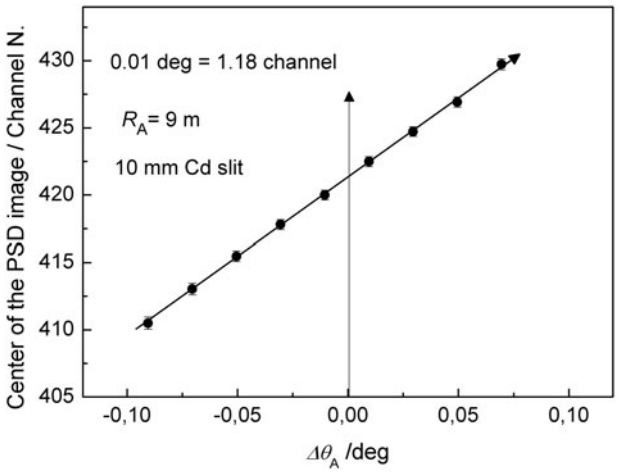

Figure 7. Linear calibration function as taken for the virgin sample laid horizontally. The width of the Cd slit was 10 mm and the bending radius $R_A = 9$ m.

material (Grade 08G2S GOST 1050) was tested. The virgin sample was submitted to shear deformation (23%) as well as to drawing deformation (23.2%). The effect of deformation on the rocking curves is documented in the results shown in Figure 5. Inspection of Figures 4 and 5 reveals that for both positions of the sample, it is possible to detect not only the effect of the elastic strains (macrostrains) resulting in a shift of the rocking curve $\Delta\theta_A$ but also the effect of plastic deformation (microstrains) resulting in a change of the diffraction profile. Peak shifts for the deformed sample in vertical ($\Delta\theta_{AV} = 0.075 \pm 0.003°$) and horizontal ($\Delta\theta_{AH} = 0.013 \pm 0.003°$) positions are different because different strain components are measured. However, peak broadening $\omega = ((FWHM_{def})^2 - (FWHM_{virg})^2)^{1/2}$ is caused by microstrains. Then, by the application of the diffraction profile analysis (Delhez *et al.*, 1982; Davydov *et al.*, 2008), information about the change of the dislocation density and the mean grain size can be obtained. However, it is clear that the method is still based on the time-consuming step-by-step analysis. Therefore, the possibility has been searched how to avoid it and to exploit somehow a position sensitive detector.

III. THREE-AXIS ALTERNATIVE EMPLOYING PSD

It has been found that for each point of $\Delta\theta_A$ in the vicinity of the peak position of the rocking curve, the diffraction profile as imaged by the PSD linearly shifts in correspondence with the value of the change of the scattering angle $2(\Delta\theta_A)$ (see Figure 6). In fact, the shift of the diffraction image is connected just with the value of $2(\Delta\theta_A)$. The range of linearity depends on $FWHM_A$ of the rocking curve. Figure 7 shows an example of this linear dependence which can be used for the calibration of $\Delta\theta_A$ against the center position of the diffraction image in the PSD which can be applied in the vicinity of the peak position of the analyzer rocking curve ($\Delta\theta_A = 0°$). It comes from the fact that the strain in the sample changes the scattering angle $2\theta_S$ by a value $\Delta(2\theta_S)$. The corresponding bunch of neutrons impinges the analyzer at some deviation $\Delta\theta_A$. As $\Delta\theta_A$ is much smaller than $FWHM_A$ of the rocking curve, the analyzer fixed at the nominal Bragg angle still diffracts the bunch (possibly with a slightly less intensity) at the deviation of the scattering angle of $2(\Delta\theta_A)$. Naturally, it results in a shift of the PSD image of the diffraction profile with respect to the strain-free position ($\Delta\theta_A = 0°$). As usual, the strains bring about a smaller effect than the $\Delta\theta_A$-span of the calibration function; therefore, it can be used for macrostrain scanning as, e.g., in the samples subjected to a thermomechanical load. Furthermore, it has been found that the strain resolution derived from the calibration function depends on the curvature of the analyzer as well as the width of the slit for the incident beam on the sample laid in the horizontal position. These properties are documented in Figures 8 and 9 for the radius of curvature $R_A = 3.6$ m and the widths of the slit at 10 and 5 mm, respectively. However, as can be seen, it has practically no effect on the determination of the elastic strain observed in the deformed sample (the difference in the peak position is within the experimental error). Nevertheless, the change of the line inclination due to the plastic deformation deserves further studies. For evaluation of the obtained data in our case, it is possible to use simple formulae $\Delta\theta_A \approx -\Delta(2\theta_S)$ for large values of R_A and $\Delta\theta_A \approx -\Delta(2\theta_S)\cdot(1 + 1/(R_A \cdot \sin\theta_A))$ for smaller values of R_A from which the change of the lattice spacing of the sample can be determined by means of the relation $\Delta\theta_S = -(\Delta d_S/d_{0,S})\cdot\tan\theta_S$.

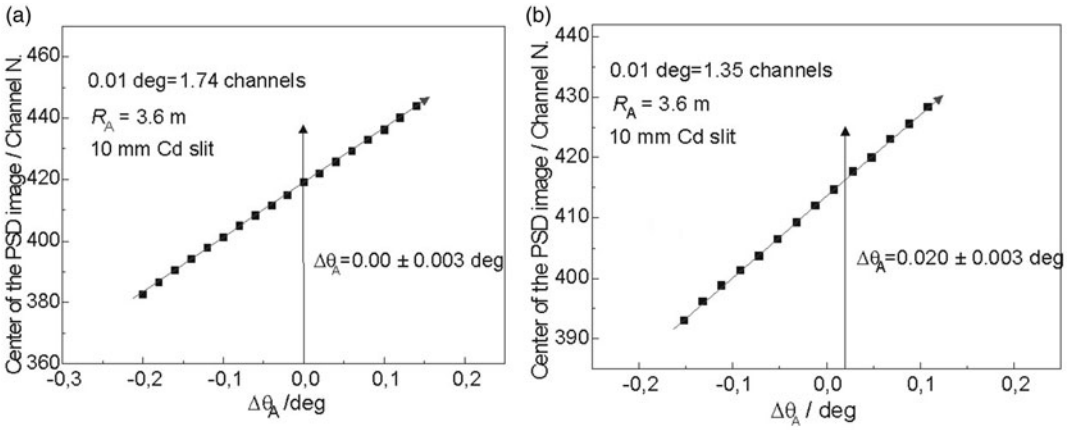

Figure 8. Linear calibration functions as taken for the virgin sample (a) and the deformed one (b) both laid horizontally. The width of the Cd slit was 10 mm and the bending radius $R_A = 3.6$ m.

https://doi.org/10.1017/S0885715620000329 Published online by Cambridge University Press

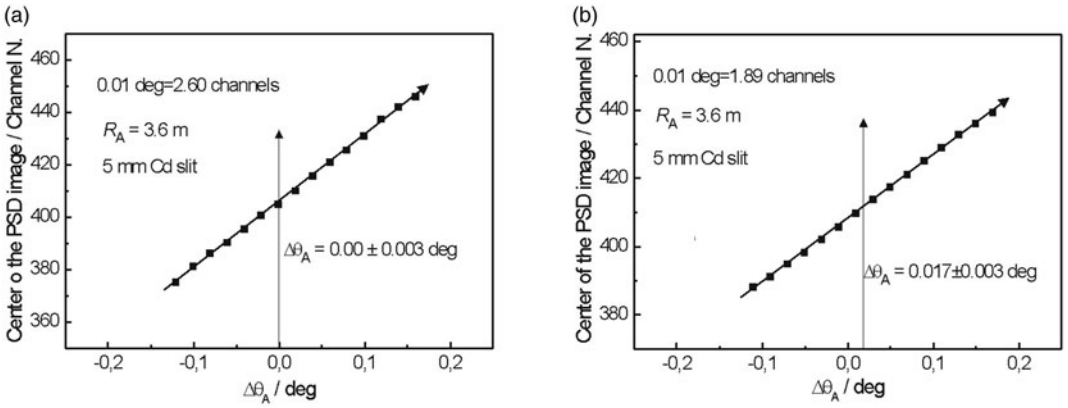

Figure 9. Linear calibration functions as taken for the virgin sample (a) and the deformed one (b) both laid horizontally. The width of the Cd slit was 5 mm and the bending radius R_A = 3.6 m.

IV. SUMMARY

The feasibility of using the high-resolution three-axis diffractometer performance in some special cases of strain/stress analysis of bulk samples of the width of 5–10 mm is presented. This measurement alternative can be utilized, namely, in the case of samples subjected to thermo-mechanical load when the position of the sample is fixed. Otherwise, for the comparison of different samples, attention should be paid to keeping the central point of the irradiated gauge volume in the same position with a high accuracy to avoid an additional error to $\Delta(2\theta_S)$ as well as to $\Delta\theta_A$. We hope that the presented neutron diffraction settings can offer an additional support to complement the information achieved by using the other conventional characterization methodologies.

ACKNOWLEDGEMENTS

Measurements were carried out at the CANAM infrastructure of the NPI CAS Řež supported through MŠMT project no. LM2015056. The presented results were also supported in the frame of the following MŠMT projects: LM2015048 and the infrastructural one – "Experimental nuclear reactors LVR-15 and LR-0." We thank Ms. B. Michalcová for a significant help in the measurements and basic elaboration of the data.

Davydov, V., Lukáš, P., Strunz, P., and Kužel, R. (**2008**). "Single-line diffraction profile analysis method used for evaluation of microstructural parameters in the plain ferritic steel upon tensile straining," Mater. Sci. Forum **571–572**, 181–188.

Delhez, R., de Keijser, T. H., and Mittemeijer, E. J. (**1982**). "Determination of crystallite size and lattice distortions through X-ray diffraction line profile analysis," Fresenius' Z. Anal. Chem. **312**(1), 1–16.

Hirschi, K., Ceretti, M., Lukáš, P., Ji, N., Braham, C., and Lodini, A. (**1999**). "Microstrain measurement in plastically deformed austenitic steel," Textures Microstruct. **33**, 219–230.

Hutchings, M. T. and Krawitz, A. D. (Eds.) (**1992**). *Measurement of Residual and Applied Stress Using Neutron Diffraction*. NATO ASI Series, Vol. 216 (Kluwer Academic Publisher, Dordrecht).

Macek, K., Lukáš, P., Janovec, J., Mikula, P., Strunz, P., Vrána, M., and Zaffagnini, M. (**1996**). "Austenite content and dislocation density in electron beam welds of a stainless maraging steel," Mater. Sci. Eng. A **208**, 131–138.

Mikula, P., Vrána, M., Lukáš, P., Šaroun, J., and Wagner, V. (**1996**). "High-resolution neutron powder diffractometry on samples of small dimensions," Mater. Sci. Forum **228-231**, 269–274.

Mikula, P., Vrána, M., Lukáš, P., Šaroun, J., Strunz, P., Ullrich, H. J., and Wagner, V. (**1997**). "Neutron diffractometer exploiting Bragg diffraction optics – a high resolution strain scanner," in *Proceedings of ICRS-5*, Vol. 2, edited by T. Ericsson, M. Odén and A. Andersson, June 16–18, 1997 (Linköping), pp. 721–725.

Noyan, I. V. and Cohen, J. B. (**1987**). *Residual Stress: Measurement by Diffraction and Interpretation* (Springer-Verlag, New York), 1st ed.

Seong, B. S., Em, V., Mikula, P., Šaroun, J., and Kang, M. H. (**2011**). "Unconventional performance of a highly luminous strain/stress scanner for high resolution studies," Mater. Sci. Forum **681**, 426–430.

Stelmukh, V., Edwards, L., Santisteban, J. R., Ganguly, S., and Fitzpatrick, M. E. (**2002**). "Weld stress mapping using neutron and synchrotron x-ray diffraction," Mater. Sci. Forum **404–407**, 599–604.

Vrána, M., Lukáš, P., Mikula, P., and Kulda, J. (**1994**). "Bragg diffraction optics in high resolution strain measurements," Nucl. Instrum. Methods Phys. Res., Sect. A **338**, 125–131.

https://doi.org/10.1017/S0885715620000329 Published online by Cambridge University Press